AIP | Journal of Applied Physics

Performance of heterojunction p+ microcrystalline silicon n crystalline silicon solar cells

M. W. M. van Cleef, J. K. Rath, F. A. Rubinelli, C. H. M. van der Werf, R. E. I. Schropp et al.

Citation: J. Appl. Phys. 82, 6089 (1997); doi: 10.1063/1.366479
View online: http://dx.doi.org/10.1063/1.366479
View Table of Contents: http://jap.aip.org/resource/1/JAPIAU/v82/i12
Published by the American Institute of Physics.

Related Articles

Efficient, bulk heterojunction organic photovoltaic cells based on boron subphthalocyanine chloride-C70
APL: Org. Electron. Photonics 5, 157 (2012)

Efficient, bulk heterojunction organic photovoltaic cells based on boron subphthalocyanine chloride-C70
Appl. Phys. Lett. 101, 033308 (2012)

CdS buffer-layer free highly efficient ZnO-CdSe photoelectrochemical cells
Appl. Phys. Lett. 101, 033906 (2012)

Transparent conductive electrodes of mixed TiO2−x–indium tin oxide for organic photovoltaics
Appl. Phys. Lett. 100, 213302 (2012)

Transparent conductive electrodes of mixed TiO2−x–indium tin oxide for organic photovoltaics
APL: Org. Electron. Photonics 5, 115 (2012)

Additional information on J. Appl. Phys.

Journal Homepage: http://jap.aip.org/
Journal Information: http://jap.aip.org/about/about_the_journal
Top downloads: http://jap.aip.org/features/most_downloaded
Information for Authors: http://jap.aip.org/authors

ADVERTISEMENT

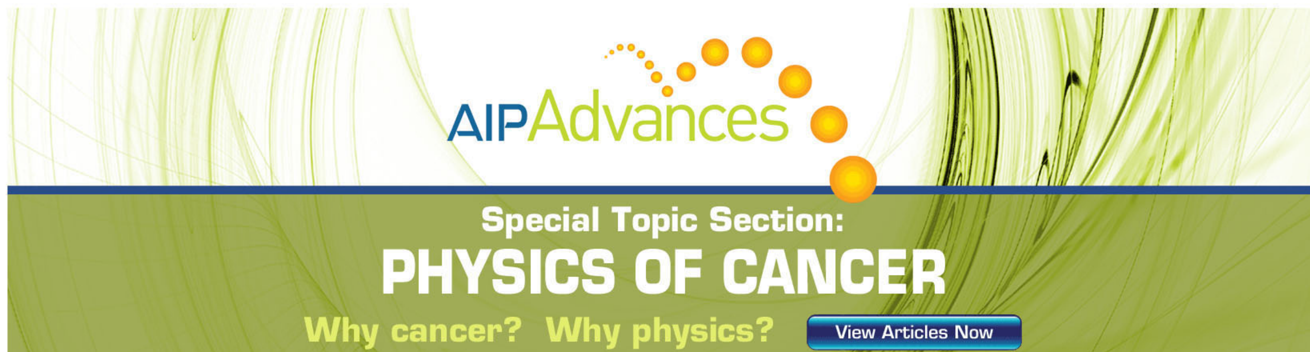

Downloaded 28 Jul 2012 to 114.70.10.202. Redistribution subject to AIP license or copyright; see http://jap.aip.org/about/rights_and_permissions

Performance of heterojunction p^+ microcrystalline silicon n crystalline silicon solar cells

M. W. M. van Cleef,[a] J. K. Rath, F. A. Rubinelli,[b] C. H. M. van der Werf, R. E. I. Schropp, and W. F. van der Weg
Utrecht University, Debye Institute, P.O. Box 80000, NL-3508 TA, Utrecht, The Netherlands

(Received 20 December 1996; accepted for publication 12 September 1997)

We have studied by Raman spectroscopy and electro-optical characterization the properties of thin boron doped microcrystalline silicon layers deposited by plasma enhanced chemical vapor deposition (PECVD) on crystalline silicon wafers and on amorphous silicon buffer layers. Thin 20–30 nm p^+ μc-Si:H layers with a considerably large crystalline volume fraction ($\sim$22%) and good window properties were deposited on crystalline silicon under moderate PECVD conditions. The performance of heterojunction solar cells incorporating such window layers were critically dependent on the interface quality and the type of buffer layer used. A large improvement of open circuit voltage is observed in these solar cells when a thin 2–3 nm wide band-gap buffer layer of intrinsic a-Si:H deposited at low temperature ($\sim$100 °C) is inserted between the microcrystalline and crystalline silicon [complete solar cell configuration: Al/$(n)c$-Si/buffer/$p^+\mu$c-Si:H/ITO/Ag)]. Detailed modeling studies showed that the wide band-gap a-Si:H buffer layer is able to prevent electron backdiffusion into the p^+ μc-Si:H layer due to the discontinuity in the conduction band at the amorphous-crystalline silicon interface, thereby reducing the high recombination losses in the microcrystalline layer. At the same time, the discontinuity in the valence band is not limiting the hole exit to the front contact and does not deteriorate the solar cell performance. The defect density inside the crystalline silicon close to the amorphous-crystalline interface has a strong effect on the operation of the cell. An extra atomic hydrogen passivation treatment prior to buffer layer deposition, in order to reduce the number of these defects, did further enhance the values of V_{oc} and fill factor, resulting in an efficiency of 12.2% for a cell without a back surface field and texturization.
© *1997 American Institute of Physics.* [S0021-8979(97)03324-0]

I. INTRODUCTION

Amorphous-crystalline silicon heterojunction solar cells have attracted increased attention after it was demonstrated that high efficiencies (21%) can be achieved on Cz silicon using a simple structure and only low temperature processes.[1] This approach has the potential of becoming a cost-effective alternative for present day c-Si and poly-Si solar cell technology.

The p-n junction in such solar cells is formed by a low temperature deposition process (plasma enhanced chemical vapor deposition: PECVD) and not by the conventional high temperature diffusion process above 900 °C. PECVD has the advantage of not only being a low temperature process, but is also a process in which the doping, band gap, and thickness of the deposited layers can be controlled and profiled accurately, which offers new opportunities for optimizing the device performance. Due to the low process temperature, cheaper lower-quality substrates (which would normally degrade in a high temperature process) can be used. Back surface fields and passivating layers can also be made by deposition. Finally, low temperature deposition will be one of the most promising options for junction formation for next generation thin film polysilicon solar cells grown on cheap substrates (e.g., glass).

Amorphous-crystalline silicon heterojunction solar cells usually consist of a thin ($<$30 nm) highly doped amorphous silicon window layer deposited on a crystalline silicon wafer of opposite doping. Apart from formation of the p-n junction, this window layer should have a high transparency (in order to maximize light absorption in the crystalline silicon base) and a high conductivity for reducing the cell's series resistance. Microcrystalline silicon could be a more suitable material as the window layer in silicon heterojunction solar cells. It possesses not only a low absorption coefficient in the blue part of the absorption spectrum but also a much higher conductivity than conventional amorphous window layers such as p^+ a-SiC:H or p^+ a-Si:H.

Highly conductive p-type microcrystalline silicon films have been obtained in the past by several groups using PECVD and other techniques,[2,3] but the deposition conditions used were often extreme (e.g., high power and high frequency), and not easily transferrable to solar cell production. Moreover, most of the claims of high conductivity are confined to thick films ($>$100 nm) which do not ensure that this property will remain at the smaller thickness employed in window layers of solar cells. It has been shown by many groups that it is difficult to achieve microcrystalline doped window layers with sufficiently small thickness ($<$20 nm).[4] This has been attributed to an incubation phase during the μc-Si:H growth which hinders the deposition of thin μc-Si:H films.[5]

In order to improve the performance of heterojunction solar cells a thin amorphous silicon buffer layer is sometimes

[a]Electronic mail: cleef@fys.ruu.nl
[b]Present address: Intec, Universidad Nacionale del Literal, Güemes, 3450, 3000 Santa Fe, Argentina.

Downloaded 28 Jul 2012 to 114.70.10.202. Redistribution subject to AIP license or copyright; see http://jap.aip.org/about/rights_and_permissions

inserted between the p layer and the crystalline silicon (the so-called HIT solar cell: heterojunction with intrinsic thin film).[6,7] The exact role of such a thin buffer layer on the operation of these solar cells is still unclear. In this paper we present a method to achieve highly conductive 20–30 nm thin p^+ μc-Si:H films on crystalline silicon at moderate PECVD deposition conditions and show the successful implementation of these window layers in crystalline silicon heterojunction solar cells. Detailed numerical simulations will be used to gain insight into the operation of these cells and to explain the observed improvement in cell performance upon incorporation of a thin buffer layer between the p^+ μc-Si:H layer and the c-Si wafer. We will finally present a new method to passivate at a low temperature the defects inside the crystalline silicon wafer close to the amorphous-crystalline interface.

II. EXPERIMENT

Boron doped μc-Si:H films were made by PECVD in an UHV multichamber deposition system[8] at the standard rf frequency (13.56 MHz), a low power density (100 mW/cm^2), and low substrate temperature (160 °C). Trimethylboron was used as the dopant gas. High hydrogen dilution ($H_2/SiH_4 = 200$) and a reduced pressure (0.99 mbar) were also necessary to maintain microcrystallinity at a small film thickness (<30 nm).[9] The microcrystallinity of these films was investigated by Raman spectroscopy measured in the backscattering geometry. The 5145 Å line of an Ar ion laser with a plasma filter was used for excitation. Films were deposited on double side polished n-type 1 Ω cm Cz c-Si wafers having a thickness of 250 μm. For optical and electrical characterization, films were also deposited on Corning 7059 glass substrates.

Heterojunction solar cells incorporating the microcrystalline layers had the following configuration: Al(200 nm)/(n)c-Si(250 μm)/buffer(0–5 nm)/(p^+)μc-Si:H(30 nm)/ITO (80 nm)/Ag grid (100 nm). A simple cell structure was chosen (without BSF, texturization, or extra antireflection coatings) and all the processing was done at low temperature (below 220 °C, i.e., substrate temperature used for the deposition of the ITO layer). Prior to deposition, the natural oxide on the wafer was removed by dipping the wafer in diluted HF (1%) for 1 min. Some (n)c-Si substrates were subjected to an extra atomic hydrogen exposure at a substrate temperature of 300 °C for 10 min prior to the buffer layer deposition. The atomic hydrogen was produced in a separate chamber of the same multichamber deposition system by flowing hydrogen gas along a hot (1800 °C) tungsten wire. In this so-called hot wire chemical vapor deposition (HWCVD)[10] technique the substrate can be exposed to atomic hydrogen without additional detrimental ion bombardment and thus can be used for passivation of surface states and of defects in the c-Si close to the surface. Three different ultrathin buffer layers were investigated: (1) device quality a-Si:H, (2) a-Si:H deposited at low substrate temperature (~100 °C), (3) a-SiC:H. The various deposition conditions of the intrinsic amorphous silicon buffer layers are listed in Table I. The transparent front contact (ITO) was deposited by reactive evaporation of an indium-tin alloy ($In_{0.9}Sn_{0.1}$) in an oxygen atmosphere (10^{-4} mbar) at a substrate temperature of 220 °C. Finally, aluminum at the back and a silver grid pattern at the front of the cell were deposited to form the contacts.

TABLE I. Deposition conditions of the investigated intrinsic amorphous silicon buffer layers.

Buffer layer	T_{sub} (°C)	p (μbar)	P_{rf} (mW/cm^2)	SiH_4:CH_4 (sccm)
Device quality a-Si:H	180	700	27	40:0
Low temp. a-Si:H	100	700	27	40:0
a-SiC:H	140	700	24	30:30

III. RESULTS AND DISCUSSION

A. Microcrystalline silicon

First we show results of the growth of microcrystalline silicon layers on crystalline silicon at moderate deposition conditions. Figure 1 shows the Raman spectrum taken of a 20 nm thin p^+-μc-Si:H layer deposited on a c-Si wafer at a pressure 0.99 mbar. The Raman signal can be deconvoluted into the pure crystalline silicon contribution from the substrate (fixed at 520 cm^{-1}), the amorphous component at 480 cm^{-1}, and the crystalline component at 514 cm^{-1} of the p^+ μc-Si:H layer. The peak position of the crystalline component of the p^+ μc-Si:H layer is shifted from the pure crystalline silicon peak position (520 cm^{-1}). No such shift is observed for thick (~300 nm) p^+-μc-Si:H layers, which have much larger grains. This suggests that the shift is caused by the grain size effect[11] and any contribution to the shift due to coupling of plasmons and phonons is negligible. The crystalline volume fraction[12] in this film was about 22%. This is well above the critical volume fraction (16%) needed for carrier transport along the percolation path.[12] This indicates that, the incubation phase is short or nonexistent. These conditions then lead to homogeneous microcrystalline growth which starts directly at the surface of the substrate

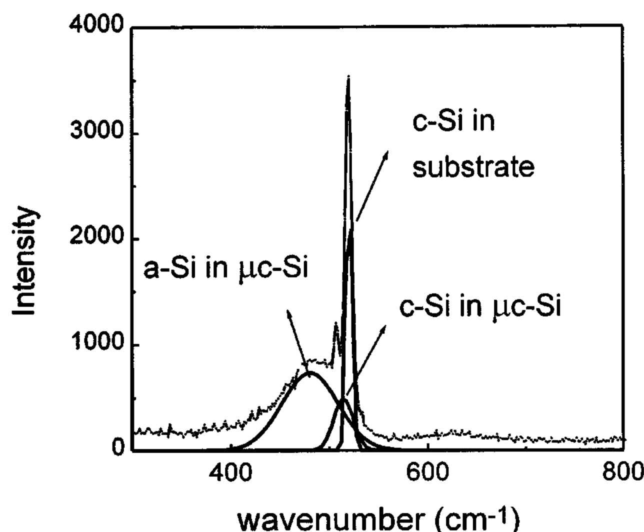

FIG. 1. Measured Raman spectrum of a 20 nm p^+ μc-Si:H layer deposited on c-Si.

Downloaded 28 Jul 2012 to 114.70.10.202. Redistribution subject to AIP license or copyright; see http://jap.aip.org/about/rights_and_permissions

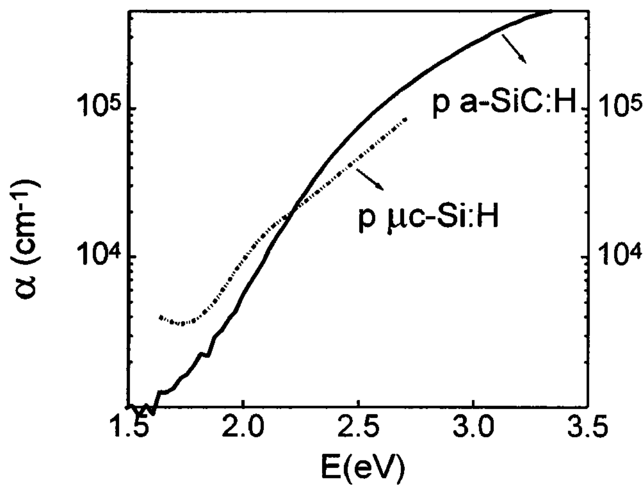

FIG. 2. Measured optical absorption coefficient as a function of energy of a p^+ μc-Si:H layer compared to a wide band-gap p^+ a-SiC:H layer, both deposited on glass.

resulting in microcrystalline layers even at small film thickness. This is confirmed by the high conductivity (3×10^{-2} S/cm) and low activation energy (0.059 eV) of a thin (15 nm) p^+ μc-Si:H film deposited on a glass substrate.[9]

Figure 2 shows the measured optical properties of the microcrystalline layers. Compared to a device-quality p^+ a-SiC:H window layer, the p^+ μc-Si:H layer has a lower absorption coefficient above 2.2 eV. In this part of the spectrum where α is above 10^4 cm^{-1}, small changes in the absorption coefficient can have a large influence on the blue response of a solar cell. This is illustrated in Fig. 3 which shows the simulated absorption as a function of wavelength for a 30 nm p layer when using different types of window layers (p^+ a-Si:H, p^+ a-SiC:H, p^+ μc-Si:H) in a standard heterojunction solar cell. The simulations were done with a ray tracing program on a multilayer structure using the optical constants (refractive index and absorption coefficient) of the separate layers as an input parameters.[13] The program also takes into account interference effects. It can be clearly observed that the absorption below 600 nm in a 30 nm p^+ μc-Si:H is considerably lower than in a p^+ a-SiC:H or p^+ a-Si:H layer of equal thickness. Assuming that all of the photogenerated carriers in the p layer are lost through recombination, as has been found experimentally,[14] the loss in short circuit current density is 1.8, 2.2, and 3.5 mA/cm^2 for a p^+ μc-Si:H, p^+ a-SiC:H, or p^+ a-Si:H layer, respectively.

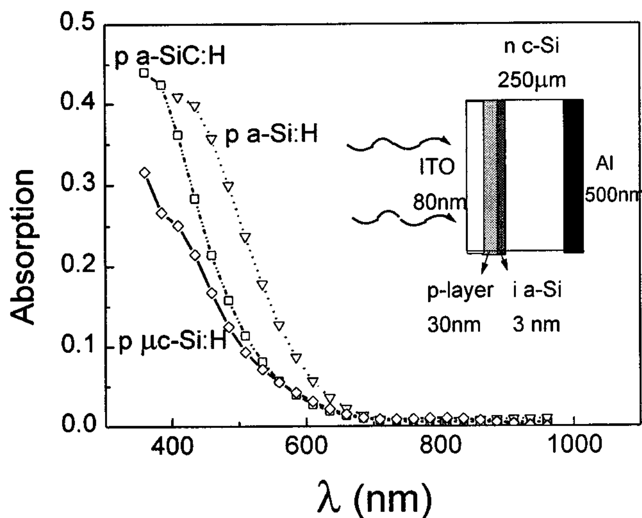

FIG. 3. Simulated absorption spectrum in the p^+ layer of a heterojunction solar cell having a standard cell configuration (80 nm ITO/30 nm p^+ layer/3 nm i-a-Si:H/250 μm (n)c-Si/500 nm Al) but different types of window layers (p^+ a-Si:H, p^+ a-SiC:H, p^+ μc-Si:H).

B. Buffer layer

The quality of a window layer can only be judged in the actual solar cell configuration. A solar cell made with a 30 nm thick p^+ μc-Si:H window layer directly deposited on the crystalline silicon wafer (no buffer layer inserted) showed very high short circuit current density J_{sc}($\sim$29 mA/cm^2), which proves the excellent window properties of the p^+ μc-Si:H layer. However, the open circuit voltage V_{oc}($\sim$0.3 V) and the fill factor FF ($\sim$0.4) of this cell were very poor. Also, the forward dark current density at low voltage was very high ($\sim5\times10^{-4}$ A/cm^2), indicating the presence of efficient recombination processes.

In order to improve the values of V_{oc} and FF, we studied the incorporation of various thin buffer layers between the c-Si and the p^+ μc-Si:H. A successful buffer layer has to fulfill three requirements: (1) it has to form a nucleation layer for μc-Si:H growth, (2) it should have a low defect density, and (3) it should passivate the surface dangling bonds on c-Si. Microcrystalline silicon layers were grown on three intrinsic amorphous silicon buffer layers: (1) device quality a-Si:H, (2) a-Si:H deposited at low temperature (100 °C), (3) a-SiC:H. Though microcrystalline silicon grows easily on c-Si substrate, it can be observed in the Raman spectrum (Fig. 4) that a film of equal thickness (30 nm) grown on device quality a-Si:H is completely amorphous in nature. This film has a very low conductivity (3×10^{-8} S/cm) and a high activation energy (0.49 eV). However, films grown under the same conditions on low temperature a-Si:H or a-SiC:H show a considerable crystalline component in the Raman spectrum. Infrared analysis and CPM studies reveal that these two amorphous (silicon) buffer layers exhibit a high microstructure factor R^* (0.5 and 0.8 for the LT a-Si:H and a-SiC:H, respectively) and large Urbach tail parameter E_0 (80 and 110 meV, respectively) compared to device-quality a-Si:H ($R^* < 0.1$ and $E_0 = 48$ meV). Apparently, the crystalline volume fraction increases when the microcrystalline layer is grown on a highly strained, void rich network.

Heterojunction solar cells incorporating the low temperature deposited a-Si:H buffer layer (2–5 nm) showed more than one order lower reverse and forward current density at low voltage compared to the cell without any buffer layer. More importantly, the cells with the 0.6–2 nm buffer layer show a large improvement in V_{oc}, i.e., from 0.35 V to over 0.50 V and to a smaller extent in fill factor, see Fig. 5. The short circuit current density (J_{sc}) remains roughly unchanged even for a 3 nm buffer layer. Due to the low deposition temperature used, the band gap of the a-Si:H is widened to 1.9 eV which reduces the optical absorption in the buffer layer compared to device-quality a-Si:H (band gap of

Downloaded 28 Jul 2012 to 114.70.10.202. Redistribution subject to AIP license or copyright; see http://jap.aip.org/about/rights_and_permissions

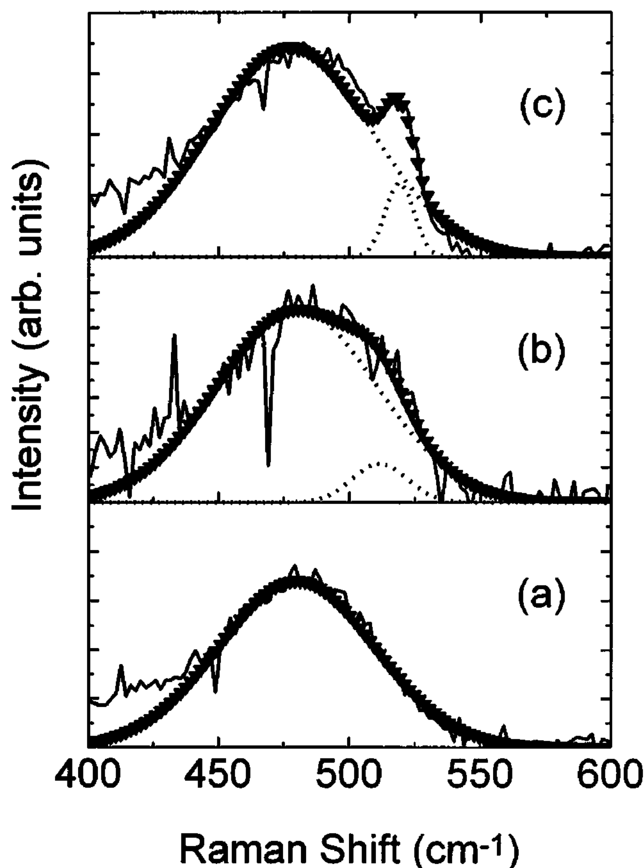

FIG. 4. Measured Raman spectra of three 30 nm thin p^+ μc-Si:H films grown on (a) device quality a-Si:H, (b) low temperature deposited a-Si:H, and (c) a-SiC:H.

1.7 eV). The application of a 2 nm buffer layer resulted in an increase of the solar cell efficiency from about 4% to nearly 9%. For thicker buffer layers (>3 nm) the low conductivity of the intrinsic a-Si:H layer becomes dominant, thereby increasing the solar cell series resistance which lowers V_{oc} and FF.

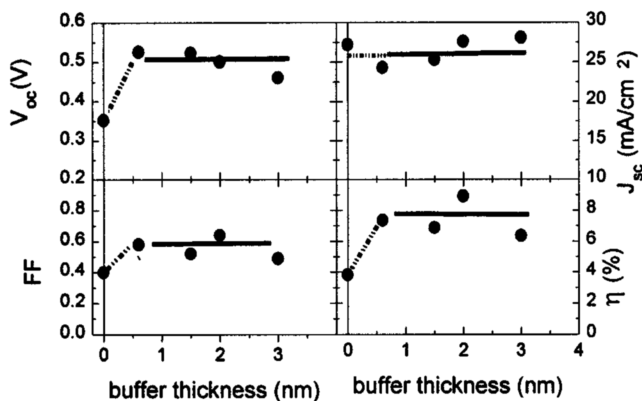

FIG. 5. Experimental light $I-V$ parameters of heterojunction solar cells having a 30 nm p^+ μc-Si:H window layer and an ultrathin low temperature deposited intrinsic a-Si:H buffer layer as a function of the buffer layer thickness. Illumination is 100 mW/cm^2 AM1.5. The cell area is 0.64 cm^2. The drawn lines are only guides to the eye.

C. Modeling

In order to gain understanding about the exact role of a buffer layer inserted between the p^+ μc-Si:H and the $(n)c$-Si layer, we employed the computer code AMPS (analysis of microelectronic and photonic structures developed at The Pennsylvania State University[15,16]) for model studies.

An overview of input parameters used in our simulations has been listed in Table II. A midgap defect density of 10^{12} cm^{-3} was adopted in the crystalline silicon wafer and an extra 5 nm thin defective layer at the top surface of the wafer has been added in order to simulate the presence of a high density of interface states. Experimentally determined values of the low temperature deposited intrinsic a-Si:H and p^+ μc-Si:H layers were taken as input parameters for the buffer and p^+ layer. The band-gap difference between the p^+ layer/buffer and buffer/c-Si was initially equally distributed between the valence and conduction band, but the effect of different distributions was also studied by adjusting the unknown electron affinity of the buffer layer. Interface defect densities in a range between 10^{10} cm^{-2} and 10^{13} cm^{-2}, and buffer layer thickness in the range of 0–5 nm were explored.

Figure 6 shows the simulated dependence of V_{oc} and J_{sc} with respect to the buffer layer thickness. We found for densities of interface states below 10^{12} cm^{-2}, in agreement with our experimental results, a significant improvement of V_{oc} upon incorporation of a thin (1–5 nm) wide-band-gap buffer layer while J_{sc} remains almost unaltered. The origin of this significant improvement of V_{oc} can be found by comparing the recombination rate profiles of the two solar cell configurations with and without a thin buffer layer. Figure 7 shows these calculated recombination rates for a forward voltage of $V=0.5$ V and under 100 mW/cm^2 illumination. Note that this plot was drawn on a log–log scale. For the cell having a 3 nm buffer layer incorporated, the recombination rate is high in the p^+ layer and at defective interface (interface defect density of 10^{11} cm^{-2}). However when no buffer is included, there is a much stronger recombination inside the p^+ layer. We have seen in our simulations that for this particular case the recombination losses surpass the photocurrent generated inside the p^+ μc-Si:H layer. Since the minority carriers, which limit the recombination in this layer, are electrons, this means that a considerable number of electrons are diffusing from the crystalline silicon into the p^+ layer and recombine there immediately. Near V_{oc} the internal electric field opposing the electron back diffusion is quite weak and the combination of a large density of defects together with a low mobility gap of the p^+ μc-Si:H layer gives rise to large recombination losses, which lowers V_{oc} significantly. The model indicates that the solar cell performance can be improved significantly by blocking or at least reducing this backdiffusion of electrons into the p^+ layer. When a wide band-gap buffer is inserted between the wafer and the p^+ μc-Si:H layer, the band discontinuity at the conduction band (ΔE_c) prevents photogenerated electrons from diffusing back into the p^+ layer, see Fig. 8. As a result, the recombination losses in the p^+ layer are strongly reduced which leads to a higher V_{oc}.

On the other hand, for voltages lower than V_{oc}, photogenerated holes coming from the crystalline silicon have no

Downloaded 28 Jul 2012 to 114.70.10.202. Redistribution subject to AIP license or copyright; see http://jap.aip.org/about/rights_and_permissions

TABLE II. List of most important input parameters used for our simulations with AMPS. For the p^+ and buffer layer experimental values of $p^+\mu$c-Si:H and low temperature deposited intrinsic a-Si:H layers were taken, respectively.

Layer	p^+ μc layer	Buffer layer	Def. interface c-Si	c-Si wafer
Thickness (nm)	30	variable	5	250 μm
Electron affinity (eV)	4.05	variable	4.05	4.05
Mobility gap (eV)	1.12	1.96	1.12	1.12
Optical gap (eV)	⋯	1.87	⋯	⋯
Doping level (cm^{-3})	4.85×10^{19}	⋯	1×10^{16}	1×10^{16}
Electron mobility (cm^2/V s)	40	20	1500	1500
Hole mobility (cm^2/V s)	4	2	480	480
Midgap defect density (cm^{-3})	5×10^{18}	5×10^{16}	variable	1×10^{12}
Valence band tail energy (meV)	50	65	⋯	⋯
Conduction band tail energy (meV)	30	45	⋯	⋯

difficulties in reaching the p^+ layer by drift diffusing over the potential barrier in the valence band. This is because the effective barrier for photogenerated holes moving towards the p^+ layer is lower than the effective barrier that electrons diffusing back into the p^+ layer have to surmount (i.e., electric field in the c-Si depletion region in addition to conduction band discontinuity). Therefore the photocurrent is not affected by the discontinuity in the valence band. Additional simulations revealed that this only holds when the discontinuity in the valence band is less than 0.45 eV. For higher valence band discontinuities the hole collection is suppressed and the current already starts decreasing at a relative low forward bias leading to S-shaped light $J-V$ characteristics and low fill factors. Since we did not observe any S-shape character or low fill factors (FF$>$0.7) in the experimental $J-V$ characteristics of our optimized heterojunction solar cells, we infer that in our devices the valence band discontinuity is less than 0.45 eV.

Since the buffer layer is quite thin ($\sim$3 nm), we also investigated the effect of direct and multistep tunneling currents flowing through the buffer layer on the illuminated $J-V$ characteristics. Preliminary modeling results show that for an equally distributed band discontinuity distribution, these mechanisms do not introduce significant changes in the $J-V$ curves predicted by AMPS. Wide band-gap buffer layers even as thin as 1.5 nm do not allow for much electron-backdiffusion into the p^+ layer.

D. Low temperature passivation

The experimental open circuit voltages of the heterojunction solar cells in the previous sections are rather low ($V_{oc}\sim$0.5 V) compared to crystalline silicon homojunction solar cells made on Cz grown silicon. From our simulation

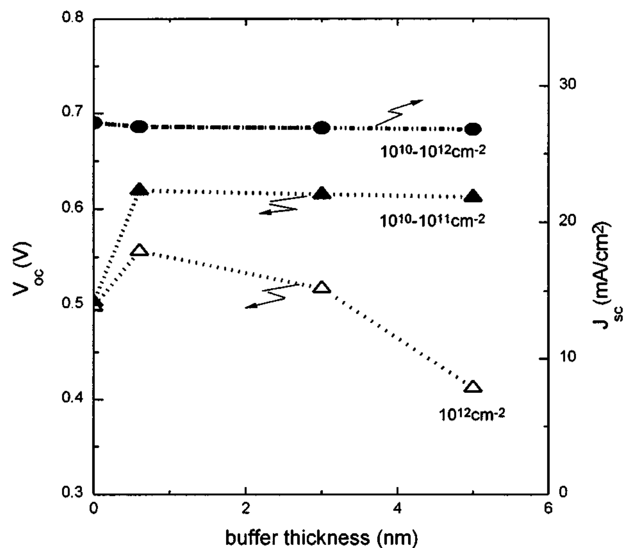

FIG. 6. Simulated dependence of open circuit voltage (V_{oc}) and short circuit current density (J_{sc}) on buffer layer thickness and interface state density for a heterojunction solar cell having the following configuration: 30 nm p^+ μc-Si:H/i a-Si:H buffer/5 nm c-Si defective interface/250 μm (n)c-Si. The band-gap difference between buffer and c-Si is equally distributed between valence and conduction band.

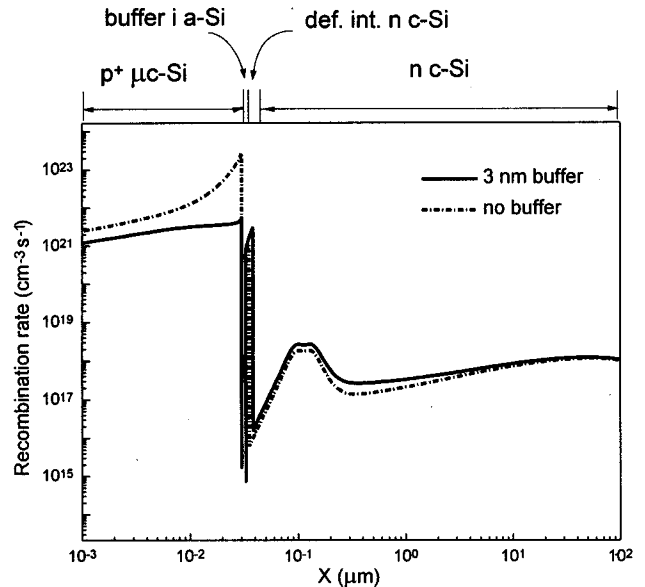

FIG. 7. Simulated recombination rate at $V=0.5$ V forward bias voltage and AM1.5 100 mW/cm^2 illumination for a heterojunction solar cell with (solid line) and without (dashed line) a 3 nm thin low temperature intrinsic a-Si:H buffer layer incorporated. The cell configuration is identical to that used for Fig. 6. The interface defect density was taken 10^{11} cm^{-2} and the band-gap difference was equally distributed over valence and conduction band.

Downloaded 28 Jul 2012 to 114.70.10.202. Redistribution subject to AIP license or copyright; see http://jap.aip.org/about/rights_and_permissions

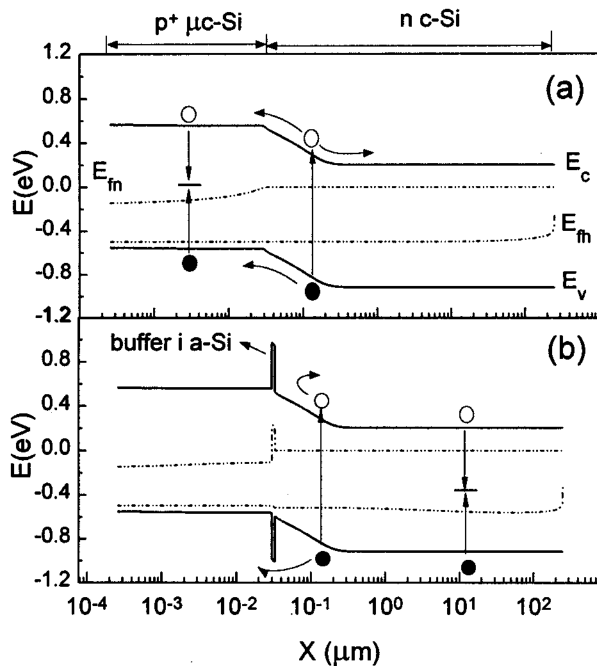

FIG. 8. Simulated band diagram at $V=0.5$ V forward bias voltage and AM1.5 100 mW/cm^2 illumination for a heterojunction solar cell (a) without and (b) with a 3 nm thin low temperature intrinsic a-Si:H buffer layer incorporated. The cell configuration is the same as for Figs. 6 and 7. The interface defect density was taken 10^{11} cm^{-2} and the band-gap difference was equally distributed over valence and conduction band.

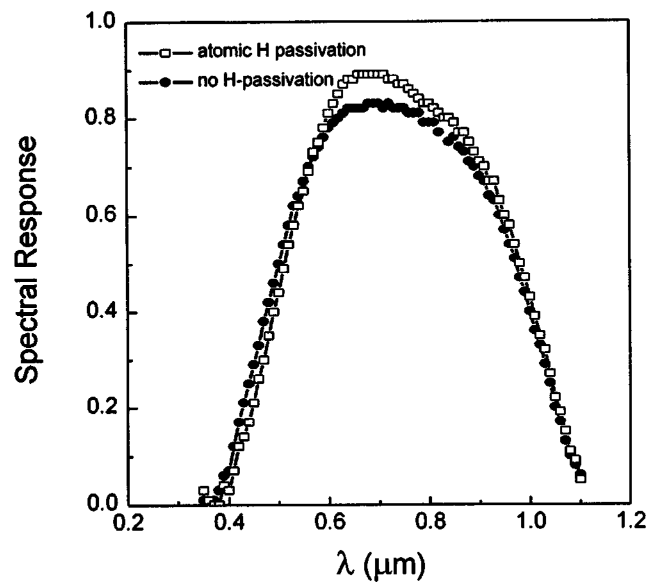

FIG. 9. Measured results of the influence of atomic hydrogen pretreatment on the spectral response for two heterojunction solar cells having identical (2 nm) thin low temperature intrinsic a-Si:H buffer layer and p^+ μc-Si:H layer (30 nm). The cell area is 0.64 cm^2. The atomic hydrogen was produced by the hot wire technique. The spectral response curves were measured at zero bias voltage and under 100 mW/cm^2 AM1.5 illumination.

studies, see Fig. 6, we conclude that V_{oc} and efficiency can be enhanced if we are able to reduce the amount of defects in the crystalline silicon close to the interface below 10^{12} cm^{-2}. Our approach was to passivate these defects by atomic hydrogen produced by the hot wire technique. It is well known that atomic hydrogen can diffuse into crystalline silicon already at low temperature (~ 300 °C) and thereby passivate dangling bonds.[17] During subsequent junction and contact formation processes, the temperature does not exceed ~ 350 °C, (i.e., the effusion temperature of hydrogen) and therefore the hydrogen is expected to remain inside the crystalline silicon.

Experimentally we found, by comparing the $J-V$ characteristics of heterojunction solar cells having identical buffer (3 nm) and p^+ layer but different pretreatment of the c-Si wafer, that an extra atomic hydrogen pretreatment of the crystalline silicon wafer prior to buffer layer deposition leads to an improvement in all the photovoltaic parameters, especially in open circuit voltage (V_{oc} from 0.50 to 0.57 V) and fill factor (FF from 0.64 to 0.73). With the atomic hydrogen pretreatment the solar cell efficiency is improved from 8.9% to 12.2%. Spectral response measurements (Fig. 9) show that the red response is significantly enhanced without much change in the blue response for the case of the H-passivated heterojunction solar cell. This indicates that more holes which are generated deep inside the crystalline silicon are collected, presumably due to lower recombination losses near the interface. This demonstrates the feasibility of the hot wire technique producing atomic hydrogen to passivate the defective surface of crystalline silicon without causing serious additional damage as is common in most H-plasma treatments.[18]

IV. SUMMARY

We have shown that thin (20–30 nm) microcrystalline layers with good window properties can be deposited at moderate PECVD conditions on crystalline silicon coated with amorphous silicon buffer layers. The performance of heterojunction solar cells incorporating such window layers was critically dependent on the type of buffer used and the quality of the interface. A large improvement in open circuit voltage is observed in these solar cells when a thin 2–3 nm wide band-gap buffer layer is inserted between the microcrystalline and crystalline silicon. Modeling studies showed that the wide band-gap a-Si:H buffer layer is able to prevent electron backdiffusion into the p^+ layer, which reduces the high recombination losses in the microcrystalline layer. An extra atomic hydrogen passivation treatment prior to buffer layer deposition, in order to reduce the number of defect states close to the interface, did further enhance V_{oc} and fill factor, resulting in an efficiency of 12.2% for a heterojunction cell without a BSF and texturization.

ACKNOWLEDGMENTS

This work is part of the priority program ''Solar Cells for the 21st Century'' funded by the Netherlands Organization for Scientific Research (NWO).

[1] T. Sawada, N. Terada, S. Tsuge, T. Baba, T. Takahama, K. Wakisaka, S. Tsuda, and S. Nakano, in *Proceedings of IEEE 1st World Conference on Photovoltaic Energy Conversion,* Hawaii, 1994 (IEEE, New York, 1994).
[2] Y. Hamakawa, Y. Matsumoto, G. Hirata, and H. Okamata, Mater. Res. Soc. Symp. Proc. **164**, 291 (1990).
[3] A. Dasgupta, S. Ghosh, and S. Ray, J. Mater. Sci. Lett. **14**, 1037 (1995).

Downloaded 28 Jul 2012 to 114.70.10.202. Redistribution subject to AIP license or copyright; see http://jap.aip.org/about/rights_and_permissions

[4] W. Luft, and Y. S. Tsuo, *Hydrogenated Amorphous Silicon Alloy Deposition Processes* (Marcel Dekker, New York, 1993).
[5] P. Roca I Cabarocas, N. Layadi, T. Heitz, B. Drevillon, and I. Solomon, Appl. Phys. Lett. **66**, 3609 (1995).
[6] H. Keppner, P. Torres, R. Flueckiger, J. Meier, A. Shah, C. Fortmann, P. Fath, K. Happle, and H. Kiess, Sol. Energy Mater. Sol. Cells **34**, 201 (1994).
[7] M. Tanaka, M. Taguchi, T. Matsuyama, T. Sawada, S. Tsuda, S. Nakano, H. Hanafusa, and Y. Kuwano, Jpn. J. Appl. Phys., Part 1 **31**, 3518 (1992).
[8] A. Madan, P. Rava, R. E. I. Schropp, and B. Von Roedern, Appl. Surf. Sci. **70/71**, 716 (1993).
[9] J. K. Rath, J. Wallinga, and R. E. I. Schropp, Mater. Res. Soc. Symp. Proc. **420**, 271 (1996).
[10] A. H. Mahan, J. Carapella, B. P. Nelson, R. S. Crandall, and I. Balberg, J. Appl. Phys. **69**, 6728 (1991).
[11] Z. Iqbal and S. Vepřek, J. Phys. C **15**, 377 (1982).
[12] R. Tsu, J. Gonzalez-Hernandez, S. S. Chao, S. C. Lee, and K. Tanaka, Appl. Phys. Lett. **40**, 534 (1982).
[13] J. Daey Ouwens, R. E. I. Schropp, J. Wallinga, and W. F. van der Weg, in *Proceedings of the 12th European Photovoltaic Solar Energy Conference*, Amsterdam, 1994, edited by R. Hill (H. S. Stephens, Bedford, UK, 1994), p. 1296.
[14] M. W. M. van Cleef, F. A. Rubinelli, J. Daey Ouwens, and R. E. I. Schropp, in *Proceedings of the 13th European Photovoltaic Solar Energy Conference*, Nice, 1995, edited by W. Freiesleben (H. S. Stephens, Bedford, UK, 1995), p. 1303.
[15] P. J. McElheley, J. K. Arch, H. S. Lin, and S. J. Fonash, J. Appl. Phys. **67**, 3803 (1990).
[16] F. A. Rubinelli, S. J. Fonash, and J. K. Arch, in *Proceedings of the 6th International Photovoltaic Science and Engineering Conference,* New Delhi, 1992, edited by B. K. Das and S. N. Singh (Oxford, New Delhi, 1992), p. 811.
[17] J. I. Pankove, Mater. Res. Soc. Symp. Proc. **262**, 309 (1992).
[18] B. L. Sopori, X. Deng, J. P. Benner, A. Rohatgi, P. Sana, S. K. Estreicher, Y. K. Park, and M. A. Roberson, Sol. Energy Mater. Sol. Cells **41/42**, 159 (1996).

Downloaded 28 Jul 2012 to 114.70.10.202. Redistribution subject to AIP license or copyright; see http://jap.aip.org/about/rights_and_permissions